Bioconjugate Chemistry

Article

pubs.acs.org/bc

Cellular Uptake and Cytotoxicity of Drug–Peptide Conjugates Regulated by Conjugation Site

Pengcheng Zhang, Andrew G. Cheetham, Lye Lin Lock, and Honggang Cui*

Department of Chemical and Biomolecular Engineering and Institute for NanoBioTechnology, Johns Hopkins University, Baltimore, Maryland 21218, United States

Supporting Information

ABSTRACT: Conjugation of anticancer drugs to hydrophilic peptides such as Tat is a widely adopted strategy to improve the drug's solubility, cellular uptake, and potency against cancerous cells. Here we report that attachment of an anticancer drug doxorubicin to the *N*- or *C*-terminal of the Tat peptide can have a significant impact on their cellular uptake and cytotoxicity against both drug-sensitive and drug-resistant cancer cells. We observed higher cellular uptake by both cell lines for *C*-terminal conjugate relative to the *N*-terminal analogue. Our results reveal that the *C*-terminal conjugate partially overcame the multidrug resistance of cervical cancer cells, while the *N*-terminal conjugate showed no significant improvement in cytotoxicity when compared with free doxorubicin. We also found that both *N*- and *C*-conjugates offer a mechanism to circumvent drug efflux associated with multidrug resistance.

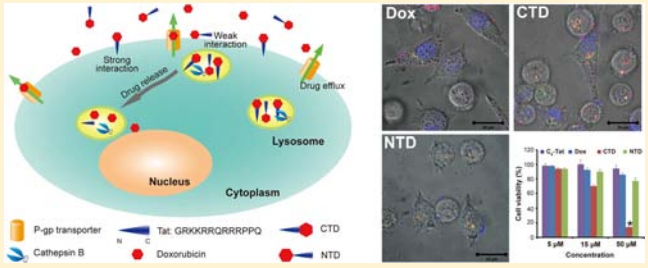

INTRODUCTION

Covalent linkage of two chemically distinct moieties into one conjugated molecule presents a facile yet effective chemistry approach to achieve new molecular characteristics and synergistic properties. Examples include the incorporation of a small auxiliary group to a biologically, electronically, or optically active segment to create self-assembling amphiphilic molecules,[1−6] and the use of polyethylene glycol (PEGylation) to reduce protein immunogenicity.[7,8] In the context of anticancer drug delivery, drug–peptide conjugates have been used as a widely adopted strategy to increase the drug's aqueous solubility,[9] to create enzyme-cleavable prodrugs,[10] to modify the drug's pharmacokinetic properties,[11] to achieve cell penetration or selectivity,[12,13] and to target a subcellular organelle.[14] Unlike the design of fusion proteins, in which the effect of fusion site (*N*- or *C*-terminal) is already under serious consideration,[15−17] the effect of conjugation site in drug–peptide conjugate design is still largely ignored, but could be very important.[18] Here we show for the first time that *N*- and *C*-terminal conjugation of an anticancer drug to the Tat cell penetrating peptide presents different cellular uptake efficiencies and thus cytotoxicity against both drug-sensitive and drug-resistant cancer cell lines.

Conjugation to cell-penetrating peptides (CPPs) presents one of the most popular and efficient techniques for achieving intracellular access.[19] Tat, the HIV transactivator of transcription protein, was the first protein found to be capable of translocating cell membranes and gaining intracellular access.[20,21] The essential protein transduction domain of the Tat protein was later found to be the peptide GRKKRRQRRRPPQ, and was subsequently named the Tat peptide.[22] Since this discovery, the Tat peptide has been conjugated to small molecules,[23] peptides,[24] proteins,[25] oligonucleic acids,[26,27] or nanoparticles[28−30] to enhance their cell membrane penetration. Although the exact cell penetration mechanism of the Tat peptide remains elusive, it is widely accepted that the interaction of the positively charged Tat peptide with negatively charged cell membrane components (such as heparin sulfate and phospholipids) is the first step of the complex process of cell penetration.[31−33] Conjugation of a cargo to the Tat peptide has been noticed to affect both the efficiency and mechanism of cell penetration by influencing the exposure and hydrophobicity of the Tat peptide,[12,34] but the influence of the conjugation site on peptide has been largely ignored. In most cases, the cargoes were conjugated at the *C*-terminal end of the Tat peptide,[22−24,26] though *N*-terminal conjugation has also been demonstrated, albeit with the use of a flexible polyethylene glycol (PEG) or GlyGly linker.[28,30,35,36] Given that most peptides are derived from key domains of proteins that also rely on the surrounding groups or free terminal to achieve the highest activity,[37,38] it is reasonable to assume that the conjugation site may affect the activity of the peptide by altering its interaction with the targeted biomolecules. It has already been reported that the *N*-terminal sequence (GRKKR) of the Tat peptide is essential for its nuclear localization,[39] and that the *N*-terminal residues of Tat peptide are also crucial in the interaction with the phospholipid-based membrane,[40] highlighting the need for

Received: November 1, 2012
Revised: February 25, 2013
Published: March 21, 2013

dx.doi.org/10.1021/bc300585h | *Bioconjugate Chem.* 2013, 24, 604−613

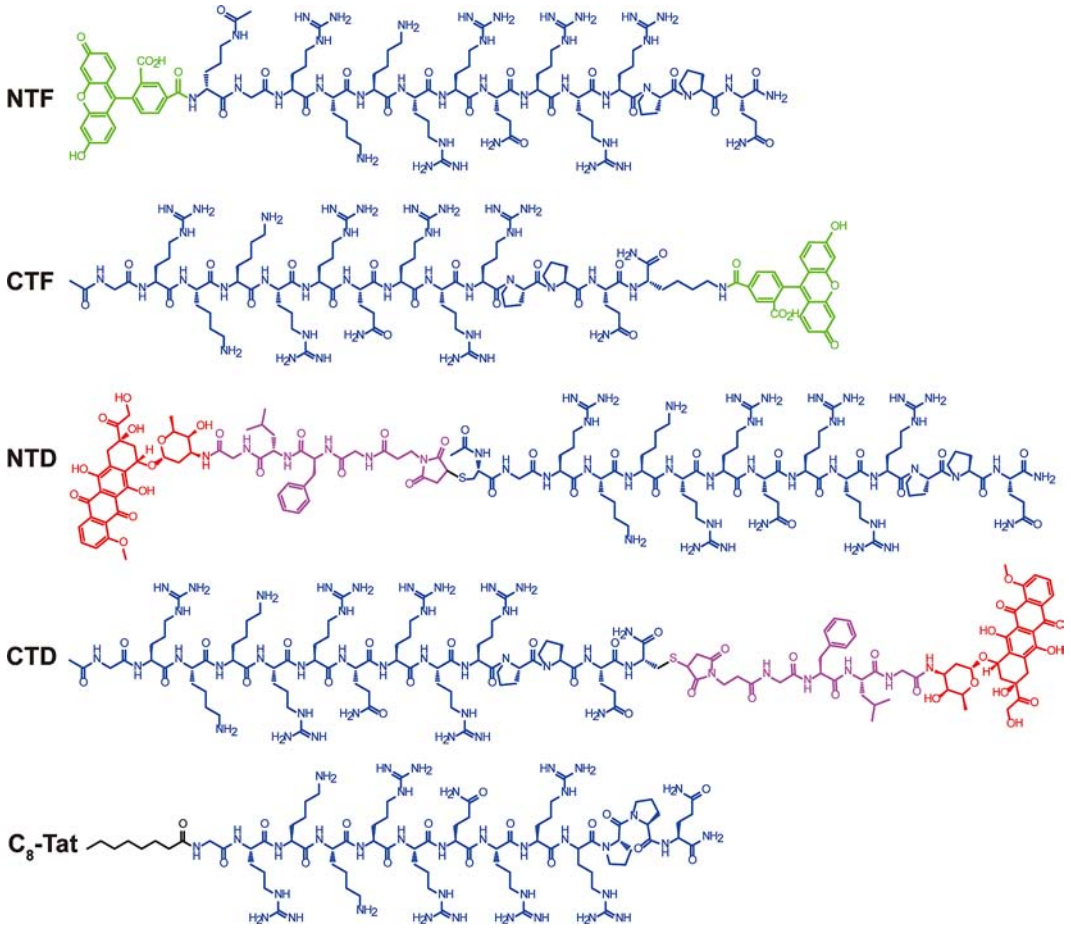

Figure 1. Chemical structures of the Tat conjugates. Chemical structures of the synthesized 5-FAM-Tat (NTF), Tat-5-FAM (CTF), doxorubicin-Tat (NTD), Tat-doxorubicin (CTD), and C_8−Tat conjugates.

careful consideration of the conjugation site locale. Even for a peptide like octaargine (R_8), a homogeneous oligomer of arginine, conjugation of the hydrophobic peptide sequence FFLIPKG to either terminal was found to significantly affect its cell penetrating efficiency.[41]

In this paper, we synthesized two pairs of *N*- and *C*-terminal Tat peptide conjugates (Figure 1) with either the fluorescent dye 5-carboxyfluorescein (5-FAM) or the anticancer drug doxorubicin (Dox), namely, 5-FAM-Tat (NTF) and Tat-5-FAM (CTF), and doxorubicin-Tat (NTD) and Tat-doxorubicin (CTD). In order to assess the toxicity of the Tat sequence, a control molecule C_8−Tat, with an octanoic hydrocarbon segment conjugated to the *N*-terminus, was also synthesized. For NTD and CTD, the enzyme-cleavable peptidic linker GFLG was incorporated to ensure that doxorubicin could be released upon endocytosis.[42−44] This GFLG tetrapeptide has been widely used as a linker in the development of polymer−drug conjugates,[45,46] and is sensitive toward the lysosomal enzyme, cathepsin B (CatB), which is present at a concentration of approximately 1 mM in the lysosome.[42] The cleavage sites of the GFLG linker were reported to be the amide bond between F and L, and also the amide bond after the C-terminal G.[47]

MATERIALS AND METHODS

Materials. All Fmoc amino acids were purchased from Advanced Automated Peptide Protein Technologies (AAPPTEC, Louisville, USA) and Rink Amide MBHA and Wang resins were purchased from Novabiochem (San Diego, CA). 5-Carboxyfluorescein (5-FAM) was purchased from AnaSpec, Inc. (Fremont, CA). Vinblastine and doxorubicin (Dox) were purchased from Avachem Scientific LLC (San Antonio, TX). Cathepsin B (bovine spleen) was purchased from EMD chemicals (San Diego, USA). 3-Maleimido-propionic acid was purchased from Bachem (Torrance, CA). All other reagents were of analytical grade and used as received without further purification.

Cell Culture. KB-3-1 and KB-V1 cell lines were kindly provided by Dr. Gottesman (Center for Cancer Research, National Cancer Institute). KB-3-1 cells were grown in DMEM (Invitrogen) containing 10% fetal bovine serum (FBS, Invitrogen) and 1% of antibiotics (Invitrogen). KB-V1 was grown in the same medium supplemented with 1 μg/mL of vinblastine to maintain its multidrug resistance. Both cell types were incubated at 37 °C in a humidified incubator with a 5% CO_2 atmosphere.

Tat Conjugates Synthesis and Characterization. All peptide conjugates were synthesized using standard 9-fluorenylmethoxycarbonyl (Fmoc) solid phase synthesis techniques. The peptides Fmoc-K(Mtt)GRK$_2$R$_2$QR$_3$P$_2$Q-Rink, Fmoc-GRK$_2$R$_2$QR$_3$P$_2$QK(Mtt)-Rink, Fmoc-CGRK$_2$R$_2$QR$_3$P$_2$Q-Rink, and Fmoc-GRK$_2$R$_2$QR$_3$P$_2$QC-Rink were synthesized on a 0.25 mmol scale on the Focus XC automated peptide synthesizer (AAPPTEC, Louisville, KY). Maleimide-modified enzyme degradable linker (Mal-GFLG-Wang) was synthesized by first assembling NH_2-GFLG-Wang

dx.doi.org/10.1021/bc300585h | *Bioconjugate Chem.* 2013, 24, 604−613

on the Focus XC (0.25 mmol scale), followed by manual addition of 3-maleimido-propionic acid using HBTU/DIEA. For NTF, 5-FAM was manually coupled at the peptide *N*-terminus (after Fmoc removal) with 5-FAM/HBTU/DIEA at a ratio of 4:4:6 relative to the peptide, shaking overnight at room temperature. For CTF molecules, 5-FAM was coupled to the Lys ε-amine (after Mtt removal) with 5-FAM/HBTU/DIEA at a ratio of 4:4:6 relative to the peptide, shaking overnight at room temperature. Fmoc deprotections were performed using a 20% 4-methylpiperidine in DMF solution for 10 min and repeated once. Mtt deprotections were carried out using a mixture of TFA/TIS/DCM with a ratio of 3:5:92 for 5 min, repeating twice. Acetylation was performed on the Lys(Mtt) side chain amine of NTF and α-amino group of glycine on CTF, respectively, using a 20% acetic anhydride in DMF solution with 100 μL of DIEA, shaking for 15 min, and the coupling was repeated once. In all cases, reactions were monitored by the ninhydrin test (Anaspec Inc., Fremont, CA) for free amines. Completed peptides were cleaved from the solid support using a mixture of TFA/TIS/H_2O in a ratio of 95:2.5:2.5 for 3 h. Excess TFA was removed by rotary evaporation and cold diethyl ether was added to precipitate the crude products, which were collected and dried under vacuum overnight. C_8−Tat was synthesized using the same protocol as NTF except caprylic acid was used instead of 5-FAM.

For NTD and CTD, doxorubicin was first manually coupled to the *C*-terminal of Mal-GFLG-OH peptide with following procedure. Mal-GFLG-OH was cleaved from the resin using a mixture of TFA/TIS/H_2O (95:2.5:2.5) for 2 h. The solution was concentrated *in vacuo* and precipitated with cold Et_2O. The solid was collected and dried at 40 °C to give Mal-GFLG-OH as an off-white solid (112.5 mg, 86%) that was used without further purification. Then, Mal-GFLG-OH (50 mg, 96 μmol) and *N*-hydroxysuccinimide (27 mg, 260 μmol) were dissolved in DMF (2 mL) and cooled to 4 °C before *N*,*N*′-diisopropylcarbodiimide (28 μL, 180 μmol) was added. After 20 min, the mixture was allowed to warm to room temperature and shaken for 16 h. Doxorubicin hydrochloride (40 mg, 69 μmol) was added to the solution and DIEA (15 μL total) was added in small increments over a 2 h period, monitoring the reaction progress by HPLC. Reaction was deemed complete 30 min after the last addition and the solution was diluted with 0.1% aqueous TFA (20 mL) and extracted with DCM (3 × 25 mL). The organic extract was washed with H_2O (30 mL), brine (30 mL), dried over Na_2SO_4, and DCM removed *in vacuo*. The product was precipitated by the addition of cold Et_2O (200 mL) and stored at −30 °C overnight. The solid was collected and dried before redissolving in 10:1 DCM/MeOH. Solvents were removed *in vacuo* to give Mal-GLFG-doxorubicin as a bright red solid (59 mg, 57%). Mal-GFLG-Dox was reacted with Ac-CGRK$_2$R$_2$QR$_3$P$_2$Q-NH$_2$ or Ac-GRK$_2$R$_2$QR$_3$P$_2$QC-NH$_2$ to obtain NTD and CTD. Briefly, for NTD, Ac-CGRK$_2$R$_2$QR$_3$P$_2$Q-NH$_2$ (20 mg, 11 μmol) and Mal-GFLG-doxorubicin (6 mg, 5.6 μmol) were dissolved in a solution of 50:50 H_2O/MeCN with 48 mM sodium phosphate (500 μL, pH 6.8) and shaken overnight. The mixture was then diluted to 5 mL with 0.1% aqueous TFA. For CTD, Ac-GRK$_2$R$_2$QR$_3$P$_2$QC-NH$_2$ (10.8 mg, 5.8 μmol) and Mal-GFLG-doxorubicin (6.1 mg, 5.7 μmol) were dissolved in a solution of 50:50 H_2O/MeCN with 48 mM sodium phosphate (500 μL, pH 6.8) and shaken overnight. The mixture was then diluted to 5 mL with 0.1% aqueous TFA.

All the conjugates were purified by preparative RP-HPLC using a Varian ProStar Model 325 HPLC (Agilent Technologies, Santa Clara, CA) equipped with a fraction collector. Separations were performed using a Varian PLRP-S column (100 Å, 10 μm, 150 × 25 mm) monitoring at 480 nm (for 5-FAM and Dox conjugates) or 220 nm (for C_8−Tat). Collected fractions were analyzed by ESI-MS (LDQ Deca ion-trap mass spectrometer, Thermo Finnigan, USA) and those containing the target molecules were combined and lyophilized (FreeZone −105 °C, Labconco, Kansas City, MO), and then stored at −30 °C.

The purity of NTF and CTF was analyzed by HPLC using the following conditions: Agilent Zorbax-C_{18} column (5 μm, 4.6 × 150 mm); the flow rate was 1 mL/min, with the mobile phase starting from 5% MeCN (with 0.1% TFA) and 95% 0.1% TFA aqueous solution at 0 min to 100% MeCN (with 0.1% TFA) at 27 min, and gradient back to the initial conditions at 30 min; the monitored wavelength was 480 nm. High resolution peptide masses were determined by MALDI-TOF mass spectrometry, using an Autoflex III MALDI-TOF instrument (Bruker, Billerica, MA). Samples were prepared by depositing 1 μL of sinapinic acid matrix (10 mg/mL in 0.05% TFA in H_2O/MeCN (1:1), Sigma-Aldrich, PA) onto the target spot, and allowed to dry for 5 min. 1 μL of aqueous peptide solution (0.1% TFA) was deposited on the corresponding spot and quickly mixed with 1 μL of sinapinic acid matrix solution. Samples were irradiated with a 355 nm UV laser and analyzed in the reflection mode.

The purity of NTD and CTD was analyzed by HPLC with the following conditions: Agilent Zorbax-C_{18} column (5 μm, 4.6 × 150 mm); the flow rate was 1 mL/min, with the mobile phase starting from 75% solvent A (0.1% TFA in water) and 25% solvent B (acetonitrile containing 0.1% TFA) (0−8 min) to 25% solvent A and 75% solvent B at 14 min, and changing back to 25% B in 1 min and holding at 25% B for 5 min; the monitored wavelength was 480 nm. The retention time of the conjugates and doxorubicin were 12.1 and 8.9 min, respectively. The conjugates were characterized using an Orbitrap Velos Pro mass spectrometer (Thermo Scientific, Waltham, MA).

Circular Dichroism (CD) Measurement. To determine the peptide conformation of C_8−Tat, NTF, CTF, NTD, and CTD, the CD spectra of the two conjugates (50 μM in Dulbecco's Phosphate-Buffered Saline, DPBS) were recorded on a J-710 spectropolarimeter (JASCO, Easton, MD) from 195 to 350 nm, and the signal was converted from ellipticity (mdeg) to mean molar ellipticity per residue (deg·cm^2·dmol^{-1}·residue^{-1}). The CD spectra of the NTD and CTD (50 μM) in trifluoroethanol (TFE) were also collected with the aim of understanding the conformation that the conjugates would adopt in cell membrane. TFE was used to mimic the membrane environment[48] and is known to stabilize certain secondary structure not stable in aqueous buffer.[49,50]

CatB Catalyzed Hydrolysis. To prove that doxorubicin can be released after the endocytosis of NTD and CTD, the release of doxorubicin from NTD and CTD was evaluated using the model lysosomal enzyme CatB according to the reported method with minor modifications.[51] Briefly, 10 μL of CatB stock solution (1 × 10^4 U/L, 17 μM) was added to 940 μL phosphate buffer (pH 5.0, containing 1 mM EDTA and 25 mM L-Cys), and preactivated for 10 min at 37 °C before the addition of 50 μL of NTD or CTD (0.3 mM). 30 μL aliquots of the mixture were sampled at time points 0 min, 10 min, 30 min, 1 h, 1.5 h, 2 h, 3 h, and 4 h, flash frozen in liquid nitrogen, and

dx.doi.org/10.1021/bc300585h | *Bioconjugate Chem.* 2013, 24, 604−613

stored at −30 °C until HPLC analysis. The HPLC conditions were the same as described above for NTD and CTD.

Cellular Uptake of Tat Conjugates. To investigate if the cell penetration efficiency of the Tat conjugates would be affected by the conjugation site, the cellular uptake of the *N*-terminal Tat conjugates (NTF and NTD) and *C*-terminal Tat conjugates (CTF and CTD) were compared. KB-V1 cells were seeded onto a 24-well plate at 1×10^5 cells/well, and allowed to attach overnight. The medium was replaced with fresh medium containing the appropriate conjugate at 5 μM, and incubated with the cells for 1, 2, or 4 h. The cells were then washed with DPBS twice, trypsinized, collected, washed twice with ice cold DPBS, and finally resuspended in 300 μL DPBS. The fluorescence intensity from endocytosed 5-FAM and doxorubicin was analyzed using a FACScalibur flow cytometer (BD Biosciences, San Jose, CA) using the FL1 (530/30) and FL3 (670LP) channels, respectively.

To investigate the effect of the conjugate concentration, the cellular uptake of different concentrations of NTD and CTD by both KB-3-1 and KB-V1 cell lines were compared. Briefly, KB-3-1 and KB-V1 cells were seeded onto 24-well plate at 1×10^5 cells/well, and allowed to attach overnight. The medium was replaced with fresh medium containing 2.5, 5, and 15 μM of Dox, NTD, or CTD as required, and incubated for 2 h. The cells were then processed and analyzed as described above.

Cytotoxicity. KB-3-1 and KB-V1 cells were seeded onto 96-well plate at 5×10^3 cells/well, and allowed to attach overnight. The medium was replaced with fresh medium containing various concentrations of C_8−Tat, NTD, or CTD, and incubated for 2 h. The medium was replaced with fresh medium and incubated for a further 46 h. The cell viability was determined using the SRB method according to the manufacturer's protocol (TOX-6, Sigma, USA).

Doxorubicin Efflux. To explore the fate of the endocytosed Dox or doxorubicin conjugates, the KB-3-1 and KB-V1 cells were incubated for 2 h with 15 μM of Dox, NTD, or CTD only or followed by a further 2 h incubation with fresh medium. The cells were then processed and analyzed by flow cytometry as described above.

Subcellular Colocalization. The subcellular location of the endocytosed drugs was investigated using confocal microscopy. Briefly, KB-3-1 and KB-V1 cells were seeded onto a 8-well glass bottom plate (Labtek, Scott's Valley, CA) pretreated with type I rat tail collagen (Invitrogen) at 4×10^4 cells/well, and allowed to attach overnight. The cells were incubated with 15 μM of Dox, NTD, or CTD for 2 h. Thirty minutes before the washing step, 100 nM Lysotracker Green (Invitrogen) and 10 μg/mL Hoechst 33342 (Invitrogen) were added. The cells were then incubated in phenol red free DMEM (Corning, Tewksbury, MA) supplemented with 10% FBS and imaged using a Zeiss 510 confocal laser scanning fluorescent microscope (Frankfurt, Germany). After imaging, the cells were incubated for a further 2 h in medium. Thirty minutes before the washing step, 100 nM Lysotracker Green (Invitrogen) and 10 μg/mL Hoechst 33342 (Invitrogen, USA) were again added. The cells were then incubated with phenol red free complete DMEM, and imaged using confocal microscopy.

RESULTS

Conjugate Characterization. The purities of the five conjugates were all above 96% according to analytical HPLC analysis (Figures S1−S5). The *m*/*z* values of NTF, CTF, and C_8−Tat were observed to be 2245.863, 2245.822, and 1843.826 Da, respectively, according to the MALDI-TOF mass spectra (Figures S1−S3), in agreement with the expected exact masses of the three conjugates (2245.221 Da calculated from $C_{99}H_{156}N_{38}O_{23}$ and 1843.172 Da calculated from $C_{78}H_{146}N_{36}O_{16}$). The observed multiply charged ions of NTD and CTD indicated that the masses of the two conjugates were 2930.4879 and 2930.5133 Da (Figure S4−S5) using high resolution ESI mass spectrometry, in agreement with the expected exact mass calculated from $C_{128}H_{199}N_{43}O_{35}S$ (2930.4834 Da).

Time and Concentration Dependent Cellular Uptake. In order to obtain quantitative information on the time- and concentration-dependent cellular uptake, we first used flow cytometry to track endocytosed conjugates in live cells. Drug resistant cervical cancer cells (KB-V1) were seeded onto 24-well plates, incubated overnight, and then treated with Tat conjugates and free 5-FAM and Dox at various concentrations (2.5, 5, and 15 μM) for different periods of time (1, 2, or 4 h). False positive signals resulting from conjugates associated with the cell membrane through nonspecific electrostatic interactions were avoided because trypsinization, a necessary step to obtain the single cell suspensions for analysis, is also known to effectively remove extracellular peptides that adhere to the cell membrane.[32,52]

Time-dependent cellular uptake was evaluated by collecting flow cytometry spectra of drug-resistant KB-V1 cells treated with different molecules at three time points (1, 2, and 4 h) (Figure 2 and Figure S6). We found that the fluorescence

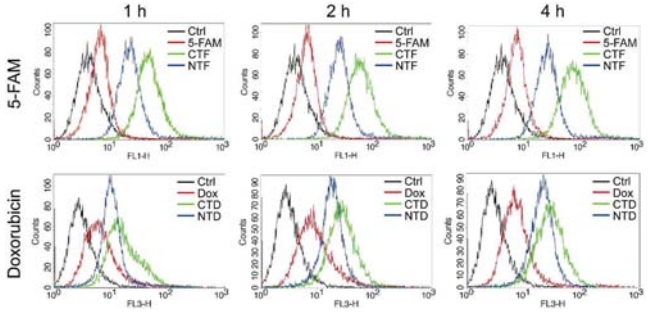

Figure 2. Representative flow cytometry spectra reveal time-dependent cellular uptake of the studied molecules by drug resistant KB-V1 cervical cancer cells. The cells studied were treated with 5 μM free 5-FAM, C-terminal Tat-5-FAM conjugate (CTF), N-terminal Tat-5-FAM conjugate (NTF), free Dox, C-terminal Tat Dox conjugate (CTD), and N-terminal Tat-Dox conjugate (NTD), respectively. The spectra were collected at three different time points (1, 2, and 4 h). Untreated cells were used as control (Ctrl).

intensity for cells treated with free 5-FAM and Dox did not change with time, while cells treated with the Tat conjugates show increased fluorescent signals with longer incubation time. These results reveal that free FAM and free Dox can quickly establish an equilibrium concentration within the drug resistant cells, most likely through a free diffusion process across the cell membrane.[53] However, their respective low fluorescent intensities suggested low accumulated concentration of the dye or drug within cells. At the same time, the increase in fluorescence intensity for Tat conjugates implies that an active cellular uptake mechanism may be involved. In both cases of 5-FAM and Dox conjugates, it is evident that the endocytosis of the *C*-terminal conjugate is always higher than its *N*-terminal analogue at each time point, clearly suggesting that the

dx.doi.org/10.1021/bc300585h | *Bioconjugate Chem.* 2013, 24, 604−613

conjugation site has a significant impact on the cellular uptake of the Tat peptide conjugates.

To investigate if the observed difference in cellular uptake between *N*-terminal conjugates and *C*-terminal conjugates is affected by drug concentration, we performed experiments on drug resistant (KB-V1) cervical cancer cells treated with Dox, NTD, and CTD at three concentrations (2.5, 5, and 15 μM). Comparative experiments were also performed on the drug sensitive (KB-3-1) cells. In these experiments, flow cytometry spectra were collected after 2 h incubation with conjugates of different concentrations. Again, the fluorescence intensity of CTD was found to be higher than that of NTD at all three concentrations in both cell lines (Figure 3), suggesting a higher

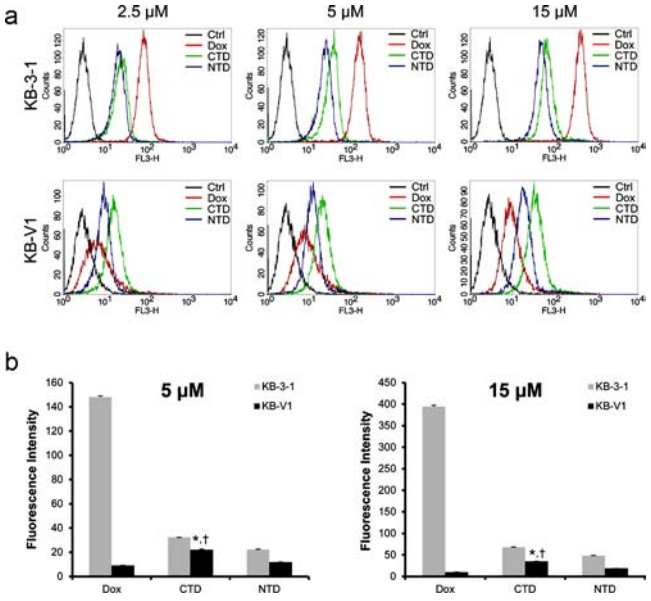

Figure 3. Concentration-dependent cellular uptake of Dox, NTD, and CTD by drug sensitive KB-3-1 and drug resistant KB-V1 cells. (a) Representative flow cytometry spectra of the cells treated with 2.5, 5, or 15 μM different drugs for 2 h, and untreated cells as control (Ctrl); (b) quantitative comparison of the fluorescence intensity (in Geo mean) in the studied two cell lines from endocytosed drugs after 2 h treatment with 5 or 15 μM drugs (* $p < 0.01$ compared with Dox, † $p < 0.01$ compared with NTD).

accumulated concentration of CTD than that of NTD. Figure 3b shows plots of the quantified fluorescence (in Geo mean) at concentrations of 5 and 15 μM conjugates, further confirming that the conjugation site has a significant impact on the efficiency of cellular uptake.

For both CTD and NTD conjugates, we observed an increase in fluorescence intensity with increasing incubation concentration for both cell lines. The drug sensitive cell line demonstrates slightly better cellular uptake than the drug resistant cell line. These results indicates that efflux proteins known to be overexpressed in the drug resistant cancer cells[54] have little effect on the Tat conjugates. In sharp contrast, the cellular uptake of Dox was found to be very efficient in KB-3-1 cells but was greatly inhibited in KB-V1 cells (Figure 3). This observation is consistent with previous reports that the overexpression of P-glycoprotein was the main mechanism behind the multidrug resistance of KB-V1 cells.[54] As a result of this efflux mechanism, the accumulated concentration of Dox is not dependent on the feeding drug concentration. This has been confirmed by our experiments (Figure 3a).

To understand if the observed difference in cellular uptake between *N*- and *C*-terminal conjugates arises from any conformational change caused by the different conjugate sites (as reported in the literature that conjugation of a cargo to a peptide may alter the secondary structure of the peptide[55]), we performed circular dichroism (CD) experiments on both the *N*- and *C*-terminal doxorubicin conjugates in Dulbecco's Phosphate-Buffered Saline (DPBS). These studies reveal that NTD and CTD adopt the same conformation in DPBS (Figure S7), with both CD spectra showing a strong negative signal around 200 nm. Similar CD spectra were observed for the NTF and CTF pair (Figure S8), and also for C_8—Tat (Figure S9). The observed CD spectra are similar to that of the extended poly(L-proline) II (PPII)-like conformation.[56−58] It was proposed that Tat peptide can insert into the cell membrane,[40] so the cellular uptake through conjugation membrane insertion may be different if the two conjugates adopted different secondary structure in cell membrane. Therefore, we collected the CD spectra of NTD and CTD in TFE to mimic the hydrophobic cell membrane environment. The CD spectra of NTD and CTD in TFE were slightly different from those in DPBS (Figures S7 and S10). A negative signal at around 222 nm was observed for both conjugates indicating partially transformation from the PPII-like structure to other helical forms in the membrane mimicking environment.[48] However, there is no significant difference in the CD spectra between NTD and CTD, implying that the two conjugates adopted very similar structure during their interactions with the cell membrane. Thus, the observed difference in cellular uptake is not linked to any difference in peptide secondary structures.

Cytotoxicity. Given the significant advantage that CTD appears to have in cellular uptake, we speculate that this should be reflected by an increased potency against cancer cell lines. To assess this, we performed cytotoxicity experiments to evaluate the efficacy of the conjugates against KB-3-1 and KB-V1 cells. Since Dox is usually given as a bolus injection with a half-life of several hours,[59] we determined the short-term cytotoxicity of the drugs only.

For drug-sensitive KB-3-1 cells, free Dox exhibited the highest antitumor activity at all the drug concentrations studied (Figure 4a). At 50 μM, nearly all the cells were killed after 2 h incubation. This is as expected because Dox is known to be able to diffuse effectively across the cell membrane.[53] Consistently, CTD demonstrated higher potency relative to NTD at all three concentrations studied, with the potency difference widening as the drug concentration was increased. Cell viability at 50 μM was approximately 15% for CTD in comparison to 58% for NTD. This observation is consistent with the cellular uptake results, with free Dox having the highest accumulated concentration in the cells, followed by CTD and NTD (Figure 3)

For the drug resistant KB-V1 cells, the cytotoxicity of free Dox dropped dramatically, with no significant cytotoxicity observed even after 2 h incubation with 50 μM of free Dox (Figure 4b). In contrast, *C*-terminal Dox conjugate (CTD) showed consistent cytotoxicity against both the drug sensitive and drug resistant cell lines (14% viability in KB-V1). The cytotoxicity of NTD dropped slightly, with the cell viability increasing from 60% to 77%. This clearly suggests that the antitumor activities of the drug conjugates were not greatly affected by the overexpression of P-glycoprotein, as is the case for free Dox. Of particular note is that the drug resistance was partially overcome as 86% of KB-V1 cells were killed after

dx.doi.org/10.1021/bc300585h | *Bioconjugate Chem.* 2013, 24, 604−613

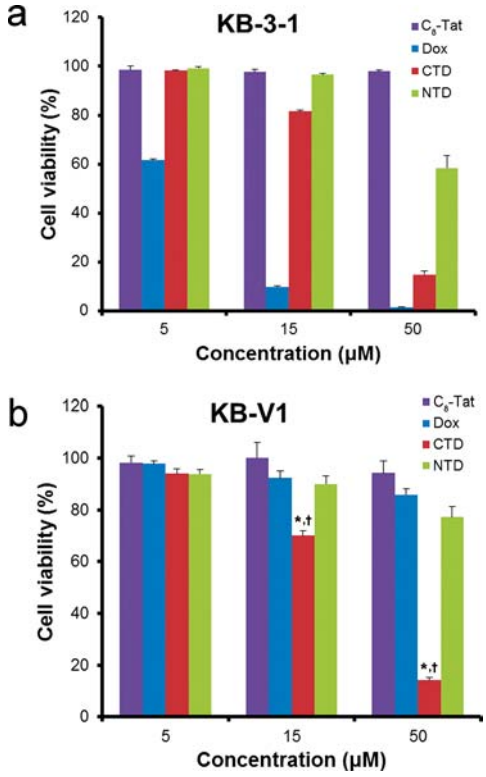

Figure 4. Cell viability of drug sensitive KB-3-1 cells (a) and resistant KB-V1 cells (b) after 2 h treatment with Dox, NTD, or CTD at three different concentrations (5, 15, and 50 μM). * $p < 0.01$ compared with Dox, † $p < 0.01$ compared with NTD.

treatment with 50 μM CTD. NTD, on the other hand, killed only 23%, showing no significant improvement in cytotoxicity compared with free Dox (14% cell death) consistent with the lower cellular accumulation observed by flow cytometry (Figure 3). It should be noted that, although advantage of CTD in cellular uptake was found in all the concentrations evaluated (Figures 2, 3, and Figure S6), only at 50 μM was significant cytotoxicity observed. This might be due to the fact that at 50 μM intracellular drug can be accumulated to a concentration sufficient to exert significant cytotoxity.

Since one key characteristic for prodrugs or drug conjugates to function against cancer cells is their successful transformation into the active drug (in our case, the free Dox can be released after the cleavage of amide bond between doxorubicin and glycine[47]),[60] it is possible that the observed difference in cytotoxicity between CTD and NTD is related to the ability of different conjugates to release free Dox. We therefore monitored the drug release from both conjugates using an HPLC method (see Materials and Methods). The drug release profiles of NTD and CTD in the presence of CatB are shown in Figure 5. Both conjugates were found to release Dox efficiently, liberating more than 50% Dox within 1.5 h, with only a slight difference in rates. The slower cleavage rate of CTD compared to NTD may result from the difference in conjugation site, as the proline residues near the *C*-terminal would introduce a bend in the structure that may decrease the affinity of the CatB for the GFLG linker in CTD and consequently the rate of cleavage. It is also possible that conjugation of the drug to different termini of the Tat moiety may exert different steric effects on the GFLG linker of the two conjugates, leading to different rates of cleavage by CatB.

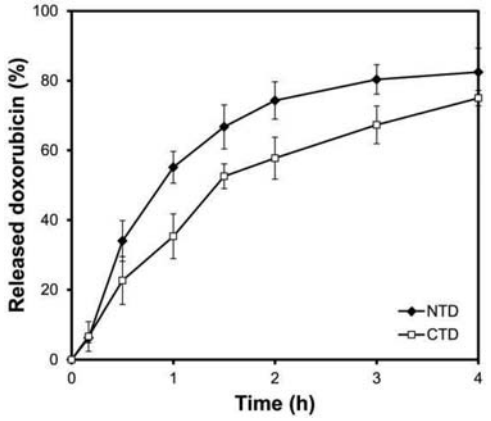

Figure 5. CatB catalyzed drug release from NTD and CTD in phosphate buffer containing 100 U/L cathepsin B (pH 5.0, 37 °C); the data are given as mean ± s.d. (n = 3). CTD shows a slightly slower release rate in comparison to NTD.

However, given the fact that the concentration of CatB within the lysosomes is on the scale of 1 mM, a concentration that is more than 5000 times higher than the concentration used here—100 U/L (equivalent of 0.17 μM active CatB)—we speculate the difference in the rate of intracellular release will be negligible for the cell experiments.

Subcellular Colocalization and Retention Ability of Conjugates. The Dox peptide conjugates with the -GFLG- linker are designed to be cleaved by CatB, a lysosomal enzyme. Hence, delivery into lysosomes is a necessary step to release the active drug. In addition, prolonged drug retention in cells could also aid in obtaining higher cytotoxicity as reported previously.[61]

Aiming to explore whether the conjugate site would affect the intracellular distribution, retention, and subsequent toxicity, we carried out confocal microscopy imaging to determine the intracellular fate of the internalized drugs. In KB-3-1 cells, an intense red fluorescence was always observed throughout the Dox treated cells, including the nucleus, suggesting that Dox can readily penetrate the cell membrane (Figure S11) and show no preference to accumulate in any subcellular organelles. In contrast, the two conjugates were predominantly colocalized with the lysosomes. After an additional 2 h incubation in the cell medium containing no drug or conjugates, cells that were initially treated with Dox showed reduced fluorescence intensity, while those treated with the conjugates displayed little change.

In drug resistant KB-V1 cells (Figure 6), a dim red fluorescence was observed only on the membrane of Dox treated cells, while a much stronger signal was observed in cells that were treated with the conjugates, again showing colocalization with the lysosomes. After a further 2 h incubation in the medium without drugs, no discernible free Dox was left in the cells, whereas no significant drop in the conjugate fluorescence intensity was observed. In both cell lines, CTD showed higher accumulation in the cells compared with NTD. The localization of the conjugates within the lysosomes should ensure the release of free doxorubicin after internalization, a prerequisite for the exhibition of cytotoxicity.

Since prolonged retention could be another mechanism by which the conjugates overcame the drug resistance of KB-V1, we quantified the retention of Dox, NTD, and CTD in both cell lines using flow cytometry (Figure 7). In these experiments,

dx.doi.org/10.1021/bc300585h | *Bioconjugate Chem.* 2013, 24, 604−613

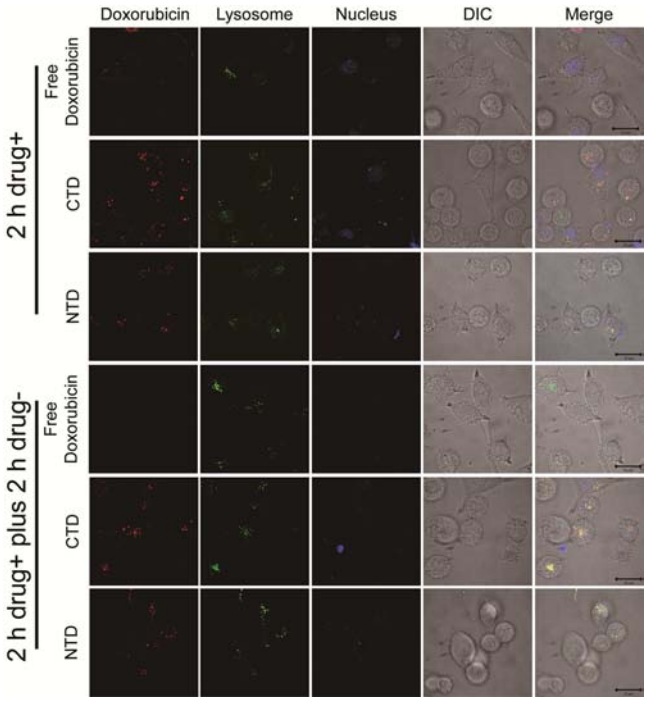

Figure 6. Subcellular colocalization of Dox, CTD, or NTD (red) in KB-V1 cells with lysosome (green, Lysotracker Green) and nucleus (blue, Hoechst 33342) after 2 h drug (15 μM) incubation or another 2 h incubation in drug free medium. Scale bar: 20 μm. An enlarged image is also included in the Supporting Information (Figure S12).

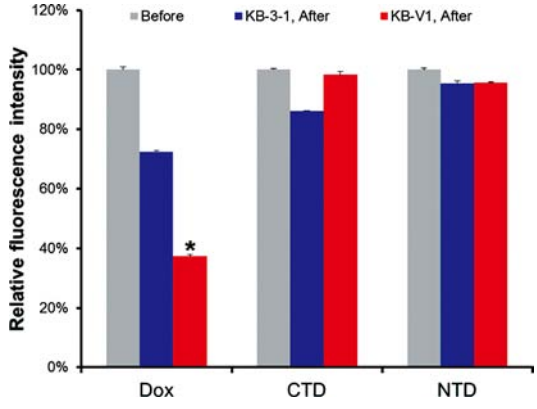

Figure 7. Retention of Dox, CTD, or NTD in drug pretreated (15 μM, 2 h) sensitive KB-3-1 and resistant KB-V1 cells after 2 h incubation in drug free medium. The fluorescence intensity collected after additional 2 h incubation in drug free medium is normalized on the basis of the fluorescence collected in pretreated cells. * $p < 0.01$ compared with KB-V1 cells before their 2 h incubation in fresh medium.

cells were first treated with 15 μM Dox, NTD, or CTD for 2 h, and then divided into two groups. Dox fluorescence was collected directly using flow cytometry for the first group with the same method described earlier. Cells of the second group were incubated in fresh medium for another 2 h. Fluorescence data were collected afterward and normalized on the basis of the corresponding fluorescence from the first group.

Immediately after 2 h drug incubation, in KB-3-1 cells, Dox showed the highest cellular uptake, approximately five and eight times that of CTD and NTD, respectively (consistent with results in Figure 3b). In the resistant KB-V1 cells, CTD showed the highest cellular accumulation, three and two times that of Dox and NTD, respectively (consistent with results in Figure 3b). However, Figure 7 clearly shows that there is a significant drop in the observed fluorescence of free Dox for both KB-3-1 and KB-V1 cell lines after the additional two hour incubation in fresh medium, with 28% and 63% of internalized Dox effluxed out by these two cell lines, respectively. In contrast, only a slight decrease in the cellular drug accumulation was observed for both NTD and CTD. There is also no discernible difference in retention between two cell lines, demonstrating that conjugation to the Tat peptide significantly enhances the drug retention within the cells.

DISCUSSION

One of the most important parameters to assess the activity of a drug that targets an intracellular component is its ability to maintain a high intracellular concentration for a prolonged period. The accumulation of drugs within the cells is primarily determined by drug internalization, drug efflux, and drug retention. The plasma membrane enveloping cells presents a major challenge for the intracellular delivery of cargo, and the overexpression of efflux transporters such as P-glycoprotein, as occurs when cells acquire multidrug resistance, makes this even more problematic.[62,63] Most widely used chemotherapeutics (e.g., paclitaxel, doxorubicin, and vinblastine) that penetrate the lipid membrane and are substrates of the transporter can be readily pumped out, preventing any significant intracellular accumulation that would otherwise lead to cell death.[64] Since the high dosages required to overcome this would unfortunately always be accompanied by serious side effects, the development of strategies for membrane translocation in both drug-sensitive and resistant cells is of critical importance.

The motivations for conjugating anticancer drugs to a peptide segment are to promote drug internalization, to circumvent the drug efflux, and to maintain a sufficient drug concentration within cells. In the special case of conjugating the Tat peptide to Dox, our experimental results clearly suggest that the Tat peptide has a significant impact on the intracellular accumulation of the resulting Dox conjugates in both drug sensitive and drug resistant cell lines.

First of all, our cellular uptake experiments for the drug sensitive KB-3-1 cell line (Figure 3b) clearly suggest that conjugation of doxorubicin to Tat peptide does not improve its internalization into cells. Rather, it reduces the ability of Dox to diffuse across the cell membrane. Similar results were observed when the cellular uptake of free doxorubicin and doxorubicin–CPP conjugates on sensitive MCF-7 cells were compared.[65] According to the subcellular colocalization experiment (Figure 6 and Figure S11), the internalized conjugates were colocalized with the lysosomes, an organelle also observed colocalizing with other Tat conjugates,[66] in stark contrast to free Dox. This observation reveals that conjugation to Tat alters the internalization pathway of Dox from passive diffusion to endocytosis. This endocytosis pathway is apparently a less efficient process than the free diffusion of Dox, thus reducing the cellular uptake of the conjugates. However, when 5-FAM, a nonmembrane penetrating dye, was conjugated to the Tat sequence, an improved internalization rate was observed both in KB-V1 cells and sensitive MCF-7 breast cancer cells (Figures S6 and S13).

Second, Tat conjugation provides a mechanism to overcome the multidrug resistance. For the drug resistant KB-V1 cell line, the intracellular accumulation of the conjugates was comparable to that in KB-3-1 cells, while a dramatic decrease in intracellular

dx.doi.org/10.1021/bc300585h | Bioconjugate Chem. 2013, 24, 604–613

accumulation was observed for Dox (Figure 3) which predominantly accumulated in the cell membrane (Figure 6). This indicates that the Dox was effluxed out by the overexpressed P-glycoprotein during its diffusion across the membrane while the accumulation of the conjugates was barely affected (Figure 8).

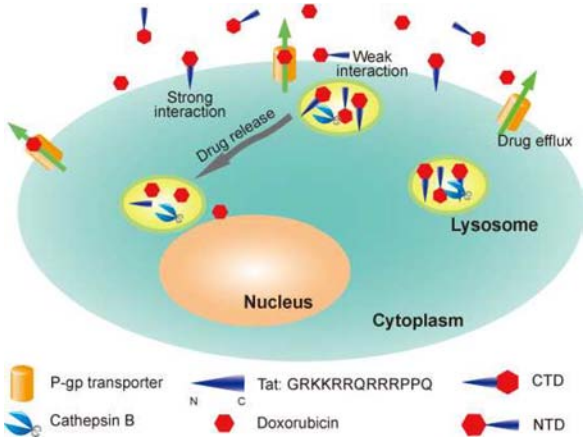

Figure 8. Schematic illustration of the proposed mechanism of CTD overcoming the multidrug resistance of KB-V1 cervical cancer cells. CTD displays a stronger interaction than NTD with the cell membrane, increasing its cellular uptake, and cannot be effluxed by the P-glycoprotein transporter—the key protein responsible for multidrug resistance—thus achieving high intracellular accumulation. Free doxorubicin can be then released from conjugate by CatB cleavage within the lysosome to exert anticancer activity in a concentration-dependent manner.

Third, Tat conjugation leads to a prolonged drug retention within cells. Prolonged retention of drug in cancer cells is another property affecting its cytotoxicity.[61] The intracellular free Dox decreased quickly after 2 h incubation in drug free medium (Figures 6, 7, and S11), indicating that Dox can diffuse out (in KB-3-1 cells) and be pumped out (in KB-V1 cells) efficiently (Figure 8). In sharp contrast, the two conjugates showed prolonged retention (Figures 6, 7, and Figure S11), suggesting that the conjugation of Tat to Dox reduces its passive diffusion across the membrane and prevents their active efflux as the modified drugs are no longer the substrates of the transporter (Figure 8).

Finally, our experiments clearly showed that the *C*-terminal conjugate, CTD, exhibited higher cellular uptake against multidrug resistant cells compared with its *N*-terminal analogue, NTD (Figures S6 and 3). There is no significant difference in the secondary structure of the two conjugates in both hydrophilic (DPBS) and hydrophobic (TFE) environments (Figures S7 and S10), indicating that conformation is not the cause of different cellular uptake. As discussed earlier, a free *N*-terminus may be crucial for some bioactive sequences to exert activity,[37,38] and more specifically, the *N*-terminal sequence of Tat peptide is very important during the interaction with lipid membrane,[40] which could trigger an adsorption-mediated endocytosis pathway.[67] *C*-terminal conjugation, by leaving the positively charged sequence exposed to the negatively charged cell membrane, seemingly possesses a higher affinity for the cells, whereas the *N*-terminal conjugation attenuates the interaction by hindering the *N*-terminal sequence (Figure 8).

Taken together, our results collectively suggest the proposed mechanism in Figure 8. Free Dox can diffuse efficiently across the cell membrane but can be readily pumped out by the P-glycoprotein, thus leading to its high accumulation and cytotoxicity in KB-3-1 but poor performance against KB-V1 cells. NTD, because of its *N*-terminal conjugation site, displays a low affinity for the cell membrane but negligible efflux by P-glycoprotein, both of which determine its low intracellular accumulation and cytotoxicity to both cell lines. CTD, a *C*-terminal Tat peptide−doxorubicin conjugate, possess a high affinity for the cell membrane and also negligible efflux by P-glycoprotein that, in combination with its efficient conversion to active doxorubicin, endow it with high cellular uptake, increased intracellular retention, and potent activity toward both drug sensitive and resistant cell lines.

CONCLUSION

In conclusion, we have demonstrated that the conjugation site can significantly affect the efficacy of the Tat−doxorubicin conjugates. Conjugating a drug to the *C*-terminal of the Tat peptide through an enzyme cleavable linker showed significantly higher cell penetration efficiency when compared with the *N*-terminal analogue. The lysosomal localization after short-term incubation ensured the cleavage of the Dox from the peptide, with CTD showing much higher cytotoxicity than Dox toward the multidrug resistant cervical cancer cell line, KB-V1, while NTD barely showed any improvement. The results here indicate that the future design and development of cell penetrating peptide conjugates should take into account the effect that the conjugation site can have on its activity.

ASSOCIATED CONTENT

Supporting Information

Additional characterization (HPLC, MALDI-TOF, and HR-ESI of the conjugates), CD spectra of the conjugates, subcellular colocalization of the drugs in KB-3-1 cells, enlarged Figure 6 (subcellular colocalization of the drugs in KB-V1 cells), and cellular uptake of CTF in MCF-7 cells. This material is available free of charge via the Internet http://pubs.acs.org.

AUTHOR INFORMATION

Corresponding Author

*Tel: (410)-516-6878. Fax: (410)-516-5510. E-mail: hcui6@jhu.edu.

Notes

The authors declare no competing financial interest.

ACKNOWLEDGMENTS

The work reported here is supported by the Johns Hopkins University (JHU) New Faculty Startup Grant, W. W. Smith Charitable Trust Medical Research Grant in Cancer, and the National Institute of Health (NIH) Postdoctoral Training Fellowship for A.C.(T-32CA130840). The authors thank Prof. K. Konstantopoulos (ChemBE, JHU), Prof. H. Mao (MSE, JHU) and Prof. K. Hristova (MSE, JHU) for the use of their respective flow cytometer, plate reader and CD spectropolarimeter. The authors also thank Dr. Jianying Zhou (SOM, JHU) for his assistance in obtaining the mass spectra of Doxorubicin conjugates.

ABBREVIATIONS

5-FAM, 5-carboxyfluorescein; CatB, Cathepsin B; CD, Circular dichroism; CPPs, Cell penetrating peptides; CTD, Tat-doxorubicin; CTF, Tat-5-carboxyfluorescein; DCM, Dichloro-

methane; DIEA, Diisopropylethylamine; DMF, *N,N*-dimethylformamide; Dox, Doxorubicin; DPBS, Dulbecco's phosphate-buffered saline; Et_2O, Ethyl ether; Fmoc, 9-fluorenylmethoxycarbonyl; HBTU, *O*-benzotrazole-*N,N,N′,N′*-tetramethyluronium hexafluorophosphate; MeCN, Acetonitrile; MeOH, Methanol; Mtt, 4-methyltrityl; NTD, Doxorubicin-Tat; NTF, 5-carboxyfluorescein-Tat; PEG, polyethylene glycol; P-gp, P-glycoprotein; R8, Octaargine; TFA, Trifluoroacetic acid; TFE, Trifluoroethanol; TIS, Triisopropylsilane

REFERENCES

(1) Aida, T., Meijer, E. W., and Stupp, S. I. (2012) Functional supramolecular polymers. *Science 335*, 813−817.

(2) Lau, C., Bitton, R., Bianco-Peled, H., Schultz, D. G., Cookson, D. J., Grosser, S. T., and Schneider, J. W. (2006) Morphological characterization of self-assembled peptide nucleic acid amphiphiles. *J. Phys. Chem. B 110*, 9027−9033.

(3) Paramonov, S. E., Jun, H. W., and Hartgerink, J. D. (2006) Self-assembly of peptide-amphiphile nanofibers: The roles of hydrogen bonding and amphiphilic packing. *J. Am. Chem. Soc. 128*, 7291−7298.

(4) Li, X. M., Kuang, Y., and Xu, B. (2012) ″Molecular trinity″ for soft nanomaterials: integrating nucleobases, amino acids, and glycosides to construct multifunctional hydrogelators. *Soft Matter 8*, 2801−2806.

(5) Smith, A. M., Williams, R. J., Tang, C., Coppo, P., Collins, R. F., Turner, M. L., Saiani, A., and Ulijn, R. V. (2008) Fmoc-Diphenylalanine self assembles to a hydrogel via a novel architecture based on pi-pi interlocked beta-sheets. *Adv. Mater. 20*, 37−41.

(6) Trent, A., Marullo, R., Lin, B., Black, M., and Tirrell, M. (2011) Structural properties of soluble peptide amphiphile micelles. *Soft Matter 7*, 9572−9582.

(7) Harris, J. M., and Chess, R. B. (2003) Effect of pegylation on pharmaceuticals. *Nat. Rev. Drug Discovery 2*, 214−221.

(8) Veronese, F. M. (2001) Peptide and protein PEGylation: a review of problems and solutions. *Biomaterials 22*, 405−417.

(9) Meyer-Losic, F., Nicolazzi, C., Quinonero, J., Ribes, F., Michel, M., Dubois, V., de Coupade, C., Boukaissi, M., Chene, A. S., Tranchant, I., Arranz, V., Zoubaa, I., Fruchart, J. S., Ravel, D., and Kearsey, J. (2008) DTS-108, a novel peptidic prodrug of SN38: in vivo efficacy and toxicokinetic studies. *Clin. Cancer Res. 14*, 2145−2153.

(10) Kotamraj, P., Russu, W. A., Jasti, B., Wu, J., and Li, X. (2011) Novel integrin-targeted binding-triggered drug delivery system for methotrexate. *Pharm. Res. 28*, 3208−3219.

(11) Sugahara, K. N., Teesalu, T., Karmali, P. P., Kotamraju, V. R., Agemy, L., Girard, O. M., Hanahan, D., Mattrey, R. F., and Ruoslahti, E. (2009) Tissue-penetrating delivery of compounds and nanoparticles into tumors. *Cancer Cell 16*, 510−520.

(12) Jones, A. T., and Sayers, E. J. (2012) Cell entry of cell penetrating peptides: tales of tails wagging dogs. *J. Controlled Release 161*, 582−591.

(13) DeFeo-Jones, D., Garsky, V. M., Wong, B. K., Feng, D. M., Bolyar, T., Haskell, K., Kiefer, D. M., Leander, K., McAvoy, E., Lumma, P., Wai, J., Senderak, E. T., Motzel, S. L., Keenan, K., Van Zwieten, M., Lin, J. H., Freidinger, R., Huff, J., Oliff, A., and Jones, R. E. (2000) A peptide-doxorubicin 'prodrug' activated by prostate-specific antigen selectively kills prostate tumor cells positive for prostate-specific antigen in vivo. *Nat. Med. 6*, 1248−1252.

(14) Pereira, M. P., and Kelley, S. O. (2011) Maximizing the therapeutic window of an antimicrobial drug by imparting mitochondrial sequestration in human cells. *J. Am. Chem. Soc. 133*, 3260−3263.

(15) Brieger, A., Plotz, G., Hinrichsen, I., Passmann, S., Adam, R., and Zeuzem, S. (2012) C-terminal fluorescent labeling impairs functionality of DNA mismatch repair proteins. *PLoS ONE 7*, e31863.

(16) Han, W., Rhee, J. S., Maximov, A., Lin, W., Hammer, R. E., Rosenmund, C., and Sudhof, T. C. (2005) C-terminal ECFP fusion impairs synaptotagmin 1 function: crowding out synaptotagmin 1. *J. Biol. Chem. 280*, 5089−5100.

(17) Weinheimer, I., Boonrod, K., Moser, M., Zwiebel, M., Fullgrabe, M., Krczal, G., and Wassenegger, M. (2010) Analysis of an autoproteolytic activity of rice yellow mottle virus silencing suppressor P1. *Biol. Chem. 391*, 271−281.

(18) Behanna, H. A., Donners, J. J. J. M., Gordon, A. C., and Stupp, S. I. (2005) Coassembly of amphiphiles with opposite peptide polarities into nanofibers. *J. Am. Chem. Soc. 127*, 1193−1200.

(19) Koren, E., and Torchilin, V. P. (2012) Cell-penetrating peptides: breaking through to the other side. *Trends Mol. Med. 18*, 385−393.

(20) Frankel, A. D., and Pabo, C. O. (1988) Cellular uptake of the Tat protein from human immunodeficiency virus. *Cell 55*, 1189−1193.

(21) Green, M., and Loewenstein, P. M. (1988) Autonomous functional domains of chemically synthesized human immunodeficiency virus Tat trans-activator protein. *Cell 55*, 1179−1188.

(22) Vives, E., Brodin, P., and Lebleu, B. (1997) A truncated HIV-1 Tat protein basic domain rapidly translocates through the plasma membrane and accumulates in the cell nucleus. *J. Biol. Chem. 272*, 16010−16017.

(23) Wang, J. T. W., Giuntini, F., Eggleston, I. M., Bown, S. G., and MacRobert, A. J. (2012) Photochemical internalisation of a macromolecular protein toxin using a cell penetrating peptide-photosensitiser conjugate. *J. Controlled Release 157*, 305−313.

(24) Boisguerin, P., Redt-Clouet, C., Franck-Miclo, A., Licheheb, S., Nargeot, J., Barrere-Lemaire, S., and Lebleu, B. (2011) Systemic delivery of BH4 anti-apoptotic peptide using CPPs prevents cardiac ischemia-reperfusion injuries in vivo. *J. Controlled Release 156*, 146−153.

(25) Gillmeister, M. P., Betenbaugh, M. J., and Fishman, P. S. (2011) Cellular trafficking and photochemical internalization of cell penetrating peptide linked cargo proteins: a dual fluorescent labeling study. *Bioconjugate Chem. 22*, 556−566.

(26) Moschos, S. A., Jones, S. W., Perry, M. M., Williams, A. E., Erjefalt, J. S., Turner, J. J., Barnes, P. J., Sproat, B. S., Gait, M. J., and Lindsay, M. A. (2007) Lung delivery studies using siRNA conjugated to TAT(48−60) and penetratin reveal peptide induced reduction in gene expression and induction of innate immunity. *Bioconjugate Chem. 18*, 1450−1459.

(27) Turner, J. J., Arzumanov, A. A., and Gait, M. J. (2005) Synthesis, cellular uptake and HIV-1 Tat-dependent trans-activation inhibition activity of oligonucleotide analogues disulphide-conjugated to cell-penetrating peptides. *Nucleic Acids Res. 33*, 27−42.

(28) Zhu, L., Kate, P., and Torchilin, V. P. (2012) Matrix metalloprotease 2-responsive multifunctional liposomal nanocarrier for enhanced tumor targeting. *ACS Nano 6*, 3491−3498.

(29) Tong, R., Hemmati, H. D., Langer, R., and Kohane, D. S. (2012) Photoswitchable nanoparticles for triggered tissue penetration and drug delivery. *J. Am. Chem. Soc. 134*, 8848−8855.

(30) Xiong, X. B., and Lavasanifar, A. (2011) Traceable multifunctional micellar nanocarriers for cancer-targeted co-delivery of MDR-1 siRNA and doxorubicin. *ACS Nano 5*, 5202−5213.

(31) Tyagi, M., Rusnati, M., Presta, M., and Giacca, M. (2001) Internalization of HIV-1 tat requires cell surface heparan sulfate proteoglycans. *J. Biol. Chem. 276*, 3254−3261.

(32) Madani, F., Lindberg, S., Langel, U., Futaki, S., and Graeslund, A. (2011) Mechanisms of cellular uptake of cell-penetrating peptides. *J. Biophys.*, 414729.

(33) Ferrari, A., Pellegrini, V., Arcangeli, C., Fittipaldi, A., Giacca, M., and Beltram, F. (2003) Caveolae-mediated internalization of extracellular HIV-1 tat fusion proteins visualized in real time. *Mol. Ther. 8*, 284−294.

(34) Brooks, H., Lebleu, B., and Vives, E. (2005) Tat peptide-mediated cellular delivery: back to basics. *Adv. Drug Delivery Rev. 57*, 559−577.

(35) Yong, H., Gu, Y. G., Clark, R. F., Marron, T., Ma, Z., Soni, N., Stone, G. G., Nilius, A. M., Marsh, K., and Djuric, S. W. (2005) Design, synthesis and structure-activity relationships of 6-O-arylpropargyl diazalides with potent activity against multidrug-resistant Streptococcus pneumoniae. *Bioorg. Med. Chem. Lett. 15*, 2653−2658.

(36) Liu, J. H., Zhao, Y. X., Guo, Q. Q., Wang, Z., Wang, H. Y., Yang, Y. X., and Huang, Y. Z. (2012) TAT-modified nanosilver for combating multidrug-resistant cancer. *Biomaterials 33*, 6155−6161.
(37) Biesecker, G., Harris, J. I., Thierry, J. C., Walker, J. E., and Wonacott, A. J. (1977) Sequence and structure of D-glyceraldehyde 3-phosphate dehydrogenase from bacillus-stearothermophilus. *Nature 266*, 328−333.
(38) Sun, X. X., and Wang, C. C. (2000) The N-terminal sequence (residues 1−65) is essential for dimerization, activities, and peptide binding of Escherichia coli DSbC. *J. Biol. Chem. 275*, 22743−22749.
(39) Ruben, S., Perkins, A., Purcell, R., Joung, K., Sia, R., Burghoff, R., Haseltine, W. A., and Rosen, C. A. (1989) Structural and functional characterization of human immunodeficiency virus TAT protein. *J. Virol. 63*, 1−8.
(40) Herce, H. D., and Garcia, A. E. (2007) Molecular dynamics simulations suggest a mechanism for translocation of the HIV-1 TAT peptide across lipid membranes. *Proc. Natl. Acad. Sci. U.S.A. 104*, 20805−20810.
(41) Takayama, K., Nakase, I., Michiue, H., Takeuchi, T., Tomizawa, K., Matsui, H., and Futaki, S. (2009) Enhanced intracellular delivery using arginine-rich peptides by the addition of penetration accelerating sequences (Pas). *J. Controlled Release 138*, 128−133.
(42) Teich, N., Bodeker, H., and Keim, V. (2002) Cathepsin B cleavage of the trypsinogen activation peptide. *BMC Gastroenterol. 2*, 16.
(43) Etrych, T., Kovar, L., Strohalm, J., Chytil, P., Rihova, B., and Ulbrich, K. (2011) Biodegradable star HPMA polymer-drug conjugates: Biodegradability, distribution and anti-tumor efficacy. *J. Controlled Release 154*, 241−248.
(44) Duncan, R. (2006) Polymer conjugates as anticancer nanomedicines. *Nat. Rev. Cancer 6*, 688−701.
(45) Chu, T. W., Yang, J., and Kopecek, J. (2012) Anti-CD20 multivalent HPMA copolymer-Fab' conjugates for the direct induction of apoptosis. *Biomaterials 33*, 7174−7181.
(46) Yang, N. N., Ye, Z. Y., Li, F., and Mahato, R. I. (2009) HPMA polymer-based site-specific delivery of oligonucleotides to hepatic stellate cells. *Bioconjugate Chem. 20*, 213−221.
(47) Rejmanová, P., Kopeček, J., Pohl, J., Baudyš, M., and Kostka, V. (1983) Polymers containing enzymatically degradable bonds, 8. Degradation of oligopeptide sequences in N-(2-hydroxypropyl)-methacrylamide copolymers by bovine spleen cathepsin B. *Die Makromolekulare Chemie 184*, 2009−2020.
(48) Rizo, J., Blanco, F. J., Kobe, B., Bruch, M. D., and Gierasch, L. M. (1993) Conformational behavior of Escherichia coli OmpA signal peptides in membrane mimetic environments. *Biochemistry 32*, 4881−4894.
(49) Sonnichsen, F. D., Vaneyk, J. E., Hodges, R. S., and Sykes, B. D. (1992) Effect of trifluoroethanol on protein secondary structure - an NMR and CD study using a synthetic actin peptide. *Biochemistry 31*, 8790−8798.
(50) Luo, P. Z., and Baldwin, R. L. (1997) Mechanism of helix induction by trifluoroethanol: A framework for extrapolating the helix-forming properties of peptides from trifluoroethanol/water mixtures back to water. *Biochemistry 36*, 8413−8421.
(51) Borgman, M. P., Ray, A., Kolhatkar, R. B., Sausville, E. A., Burger, A. M., and Ghandehari, H. (2009) Targetable HPMA copolymer-aminohexylgeldanamycin conjugates for prostate cancer therapy. *Pharm. Res. 26*, 1407−1418.
(52) Richard, J. P., Melikov, K., Vives, E., Ramos, C., Verbeure, B., Gait, M. J., Chernomordik, L. V., and Lebleu, B. (2003) Cell-penetrating peptides. A reevaluation of the mechanism of cellular uptake. *J. Biol. Chem. 278*, 585−590.
(53) van Lummel, M., van Blitterswijk, W. J., Vink, S. R., Veldman, R. J., van der Valk, M. A., Schipper, D., Dicheva, B. M., Eggermont, A. M. M., ten Hagen, T. L. M., Verheij, M., and Koning, G. A. (2011) Enriching lipid nanovesicles with short-chain glucosylceramide improves doxorubicin delivery and efficacy in solid tumors. *FASEB J. 25*, 280−289.
(54) Akiyama, S. I., Fojo, A., Hanover, J. A., Pastan, I., and Gottesman, M. M. (1985) Isolation and genetic characterization of human KB-cell lines resistant to multiple-drugs. *Somat. Cell Mol. Genet. 11*, 117−126.
(55) Mier, W., Zitzmann, S., Kramer, S., Reed, J., Knapp, E. M., Altmann, A., Eisenhut, M., and Haberkorn, U. (2007) Influence of chelate conjugation on a newly identified tumor-targeting peptide. *J. Nucl. Med. 48*, 1545−1552.
(56) Farrell, H. M., Wickham, E. D., Unruh, J. J., Qi, P. X., and Hoagland, P. D. (2001) Secondary structural studies of bovine caseins: temperature dependence of beta-casein structure as analyzed by circular dichroism and FTIR spectroscopy and correlation with micellization. *Food Hydrocoll. 15*, 341−354.
(57) Greenfield, N. J. (2006) Using circular dichroism spectra to estimate protein secondary structure. *Nat. Protoc. 1*, 2876−2890.
(58) Rucker, A. L., and Creamer, T. P. (2002) Polyproline II helical structure in protein unfolded states: Lysine peptides revisited. *Protein Sci. 11*, 980−985.
(59) Cao, N., and Feng, S. S. (2008) Doxorubicin conjugated to D-alpha-tocopheryl polyethylene glycol 1000 succinate (TPGS): Conjugation chemistry, characterization, in vitro and in vivo evaluation. *Biomaterials 29*, 3856−3865.
(60) Rautio, J., Kumpulainen, H., Heimbach, T., Oliyai, R., Oh, D., Jarvinen, T., and Savolainen, J. (2008) Prodrugs: design and clinical applications. *Nat. Rev. Drug Discovery 7*, 255−270.
(61) Theodossiou, T. A., Galanou, M. C., and Paleos, C. M. (2008) Novel amiodarone-doxorubicin cocktail liposomes enhance doxorubicin retention and cytotoxicity in DU145 human prostate carcinoma cells. *J. Med. Chem. 51*, 6067−6074.
(62) Persidis, A. (1999) Cancer multidrug resistance. *Nat. Biotechnol. 17*, 94−95.
(63) Dong, X. W., and Mumper, R. J. (2010) Nanomedicinal strategies to treat multidrug-resistant tumors: current progress. *Nanomedicine 5*, 597−615.
(64) Ford, J. M., and Hait, W. N. (1990) Pharmacology of drugs that alter multidrug resistance in cancer. *Pharmacol. Rev. 42*, 155−199.
(65) Aroui, S., Ram, N., Appaix, F., Ronjat, M., Kenani, A., Pirollet, F., and De Waard, M. (2009) Maurocalcine as a non toxic drug carrier overcomes doxorubicin resistance in the cancer cell line MDA-MB 231. *Pharm. Res. 26*, 836−845.
(66) Sandgren, S., Cheng, F., and Belting, M. (2002) Nuclear targeting of macromolecular polyanions by an HIV-Tat derived peptide - Role for cell-surface proteoglycans. *J. Biol. Chem. 277*, 38877−38883.
(67) Missirlis, D., Khant, H., and Tirrell, M. (2009) Mechanisms of peptide amphiphile internalization by SJSA-1 cells in vitro. *Biochemistry 48*, 3304−3314.